

Multistage, Multirate FIR Filter Structures for Narrow Transition-Band Filters

Tor A. Ramstad*

School of Electrical Engineering
Georgia Institute of Technology
Atlanta, GA 30332

Tapio Saramäki

Signal Processing Laboratory
Tampere University of Technology
P. O. Box 527, SF-33101 Tampere, Finland

Abstract— This paper presents an FIR filter system capable of implementing virtually any practical lowpass and highpass filter with as little as 50-60 multiplications per sample. The method is based on multirate techniques and complementary filters. We first give a brief presentation of the principle and the necessary building blocks. Then, practical design methods for optimization are presented together with design examples and plots of the multiplication rates. Finally, aliasing and finite wordlength effects are discussed. The resulting system, while having a remarkably low arithmetic complexity, will usually require somewhat more memory than a conventional optimum direct-form filter and a slight increase in the internal signal representations.

I. INTRODUCTION

Narrow transition-band FIR filters often require forbidding filter lengths for practical implementations. Even though IIR filters can offer significantly lower order, they suffer from shortcomings like nonlinear phase, instabilities and very large wordlength requirements for the same filter specifications, and it is therefore desirable to find alternative FIR structures that lower the processing load. Several methods have been devised to achieve this goal, most notable among these are the IFIR [1] and the multirate techniques [2] which can both be applied only to narrow- or broadband filters, and the structure suggested by Jing and Fam [3] and Lim [4] which can cope with any bandwidth. We have earlier presented a method which combines the Jing-Fam method with multirate techniques in such a way that the overall processing will be less than for IIR filters when strict transition-band requirements apply, and we have shown that the multiplication rate is limited to about 50-60 per sample for any reasonable filter specification [5].

In this paper we again present the basic principle of the method and go into finer details about the implementation strategies and optimizations. We also discuss the aliasing noise problem resulting from the multirate operations and present models and results for finite word-length effects.

II. BASIC STRUCTURES

To simplify the processing in narrow transition-band low-pass or high-pass filters we use the following strategy: Assume that the filter $H(z)$ shown in Fig. 1(a) satisfies the given specifications. We now try to replace this filter by a cascade of a two-port and a filter $H_1(z)$ as given in Fig. 1(b). It is not necessary for the new system exactly to mimic the original filter, but it must satisfy the same filter requirements. The question is now: can we find two-ports combined with the filter $H_1(z)$ which will reduce the multiplication and addition rates while limiting the necessary filter memory?

Before we explain the basic building blocks, we will adopt the terminology *narrowband* and *broadband* for filters satisfying $f_b < f_s/4$ and $f_b > f_s/4$, respectively, where f_b is the filter bandwidth and f_s is the sampling frequency.

Two fundamental building blocks will be sufficient to achieve our goal. One block transforms the problem from a narrowband to a broadband filter, while the other one does the opposite. If we manage to reduce the overall processing in going from the original

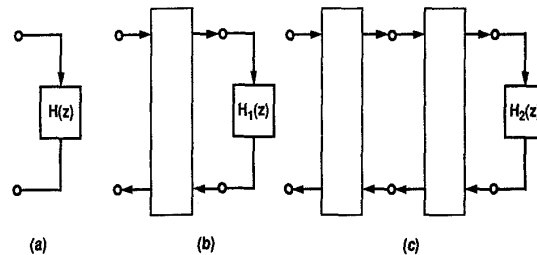


Fig. 1. Implementation of an FIR filter using two-port transforms.

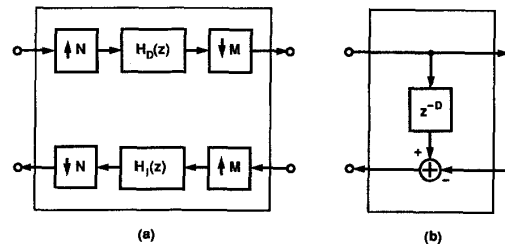


Fig. 2. Two basic building blocks for synthesizing a computationally efficient FIR filter.

filter to the system in Fig. 1(b), we can repeat the process on $H_1(z)$ leaving the system in Fig. 1(c) with terminating filter $H_2(z)$. Again a broadband filter $H_1(z)$ is turned into a narrowband $H_2(z)$ or vice versa. The process can be repeated until the processing left in the terminating filter $H_i(z)$ is negligible or the total processing in the system is minimized.

What simple two-ports can implement the low-pass to high-pass and high-pass to low-pass operations while restricting the system to remain linear phase?

A narrowband-to-broadband two-port which uses standard multirate techniques is depicted in Fig. 2(a). The decimation ratio $r = M/N$ must be selected such that it leaves the terminating filter as a broadband filter. In Fig. 3 we first show the frequency response of $H(z)$ and a ratio 2 decimation filter (i. e. $N = 1$ and $M = 2$) [Fig. 3(a)] and then the filter requirements for $H_1(z)$ [Fig. 3(b)].

Comparing $H(z)$ and $H_1(z)$ in the example above, we realize that the sampling rate in $H_1(z)$ is lowered by r and the relative transition bandwidth is increased by the same factor. Assuming that the filter length is inversely proportional to the relative transition bandwidth, we conclude that the processing in $H_1(z)$ is lowered by a factor $(M/N)^2$ as compared to $H(z)$.

The broadband-to-narrowband transformation can be implemented using a complementation technique as shown in Fig. 2(b) when the internal delay is exactly equal to the delay of the filter $H_1(z)$. Notice that this operation also performs a lowpass-to-highpass trans-

*On leave from Department of Electrical and Computer Engineering, The Norwegian Institute of Technology, N-7034 Trondheim-NTH, Norway

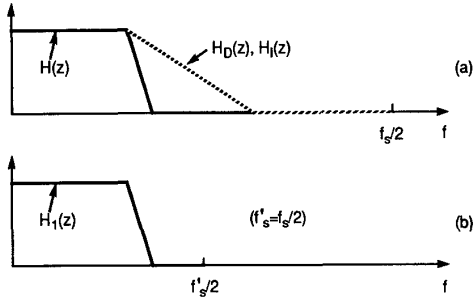


Fig. 3. Design of a narrow-band filter $H(z)$ using the building block of Fig. 2(a) with $N = 1$ and $M = 2$ and a broadband filter $H_1(z)$.

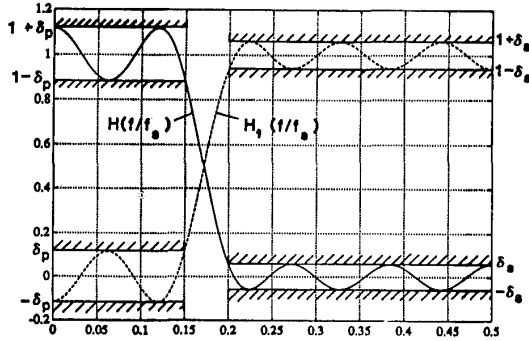


Fig. 4. Frequency response of the filter $H_1(z)$ and the complementary response obtained using the system in Fig. 1(b) with the structure in Fig. 2(b) as a two-port.

form, or vice versa. See Fig. 4. The given block requires only one addition per sample and leaves the sampling frequency unchanged.

With these building blocks our main concern in system optimization is to select good substructures for the decimation/interpolation transformations to avoid that the processing in these structures surpasses the processing in the original filter.

After studying various possible sub-structures, we have come to the conclusion that we only need two different types of decimation/interpolation two-ports, one using decimation by 2 and the other decimation by 2/3, both constructed using half-band filters as discussed in the next section.

III. HALF-BAND FILTERS

For constructing the decimation filter $H_D(z)$ and the interpolation filter $H_I(z)$, half-band filters [6] are particularly efficient. The transfer function of these filters can be written as

$$H_D(z) = \frac{1}{2}z^{-K} + G(z^2), \quad (1)$$

where K is an odd integer and the order of $G(z^2)$ is K in z^2 or $2K$ in z . When it is used for decimation or interpolation, this filter can be implemented using the commutative structures [7] shown in Fig. 5. The delay branch $z^{-(K-1)/2}$ can be shared with $G(z)$. In the decimation case, this can be done using the transposed direct-form realization exploiting the coefficient symmetry of $G(z)$. In the interpolation case, the direct-from realization is used. When the symmetry in the coefficients of $G(z)$ is exploited, we need only $(K+1)/2$ multipliers plus a trivial multiplication by 0.5 in the decimation case. Since $G(z)$ is working in both cases at the lower sampling rate of $\hat{f}_s = f_s/2$, the implementation of both $H_D(z)$ and $H_I(z)$ requires only $f_s(K+1)/2$ multiplications per second. The half-band filters are characterized by the facts that their passband

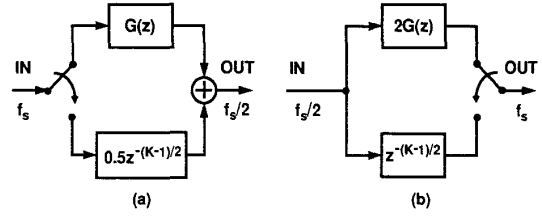


Fig. 5. Commutative structures for FIR half-band filters. (a) Decimator. (b) Interpolator. Note that in the interpolation case the filter output must be multiplied by two to preserve the signal energy.

and stopband ripples are equal and the passband and stopband edges are related via $f_{st} = f_s/2 - f_p$.

IV. DESIGN EQUATIONS

In this section, we give the basic design equations for synthesizing the proposed filters. All what is needed is to determine the conditions under which a filter $H(z)$ can be synthesized in terms of the building blocks of Section II and a termination filter which we here denote by $\hat{H}(z)$. After knowing these conditions, we are able to repeat the overall synthesis procedure. First, we concentrate on the required passband and stopband edges of the decimator and interpolator filters and those of the new termination. Let $H(z)$ be a lowpass filter with passband and stopband edges of $f_c \pm \Delta$ and sampling rate of f_s . There are the following three cases which require different constructions for $H(z)$:

Case A: $f_c < f_s/4$ and $f_c + \Delta$ is not close to $f_s/4$.

Case B: $f_c > f_s/4$ and $f_c - \Delta$ is not close to $f_s/4$.

Case C: $f_s/4$ is close to or inside the interval $[f_c - \Delta, f_c + \Delta]$.

In Case A, $H(z)$ is a narrow-band lowpass filter and we use the building block of Fig. 2(a) with $N = 1$ and $M = 2$. When this block is cascaded with the termination $\hat{H}(z)$, the relation between the z -transforms of the input signal $x(n)$ and the output signal $y(n)$ becomes

$$Y(z) = F_1(z)X(z) + F_2(z)X(-z) \quad (2a)$$

where

$$F_1(z) = \hat{H}(z^2)H_D(z)H_I(z) \quad (2b)$$

and

$$F_2(z) = \hat{H}(z^2)H_D(-z)H_I(z). \quad (2c)$$

Here, $F_1(z)$ is a conventional transfer function from the input to the output. This transfer function must satisfy the conditions stated for $H(z)$. $F_2(z)X(-z)$ is the aliased term due to the sampling rate alteration and the response of $F_2(z)$ must be small in the frequency range $[0, f_s/2]$. The desired result is obtained by selecting the edges of $\hat{H}(z)$ working at the sampling rate of $\hat{f}_s = f_s/2$ to be those of the overall filter, i.e., $\hat{f}_c \pm \Delta$ with $\hat{f}_c = f_c$. Because of the periodicity of $\hat{H}(z^2)$, it has an extra passband $[f_s/2 - (f_c - \Delta), f_s/2]$ and an extra transition band $[f_s/2 - (f_c + \Delta), f_s/2 - (f_c - \Delta)]$ (see Fig. 6). The required passband and stopband edges for $H_D(z)$ and $H_I(z)$ are

$$f_p^{(D)} = f_c - \Delta, \quad f_{st} = f_s/2 - (f_c + \Delta). \quad (3)$$

The resulting $H_D(z)$ and $H_I(z)$ preserve the first passband region of $\hat{H}(z^2)$ and attenuate the extra transition band and the extra passband of $\hat{H}(z^2)$, giving the desired response for $F_1(z)$. In the case of $F_2(z)$, $H_I(z)$ attenuates the second transition band and the second passband of $\hat{H}(z^2)$ and $H_D(-z)$ takes care of the lower ones, resulting in a small aliased term $F_2(z)X(-z)$. It has been observed experimentally that the required stopband edge of $H_D(z)$ and $H_I(z)$ can be selected to be

$$f_{st}^{(D)} = f_s/2 - (f_c + \Delta/3). \quad (4)$$

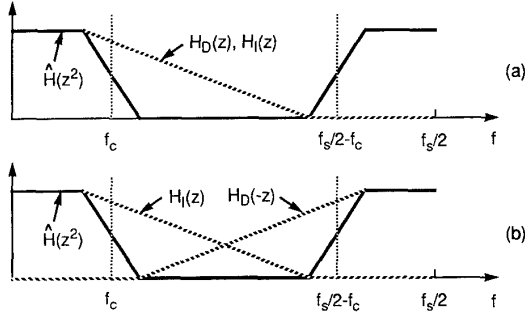


Fig. 6. Transfer functions for the aliased and unaliased components in Case A. (a) Terms in $F_1(z)$. (b) Terms in $F_2(z)$.

This is because the termination filter $\hat{H}(z^2)$ provides some attenuation in the transition bands near the stopband edges.

In Case B, $H(z)$ is a wideband design and we first use the building block of Fig. 2(b) to convert the problem to the design of narrowband highpass filter. The passband edge is $f_c + \Delta$ and the stopband edge is $f_c - \Delta$. This filter can be constructed as in Case A using the building block of Fig. 2(a) with $N = 1$ and $M = 2$. The desired result is obtained by selecting the edges of a lowpass $\hat{H}(z)$ to be $\hat{f}_c \pm \Delta$, where

$$\hat{f}_c = f_s/2 - f_c. \quad (5)$$

The required $H_D(z)$ and $H_I(z)$ are highpass filters with edges

$$f_p^{(D)} = f_c + \Delta, \quad f_{st}^{(D)} = f_s/2 - f_c + \Delta/3. \quad (6)$$

See [5] for details.

Using half-band filters with properties as discussed above, in Case A, the passband edge has to be selected as

$$f_p^{(D)} = f_c + \Delta/3 \quad (7)$$

to give the desired stopband edge. In Case B, the half-band filter is a highpass design with the stopband edge $f_{st}^{(D)}$ as given in Eq. (6).

In Case C, $f_s/4$ is either in the transition band of $H(z)$ or the passband or the stopband edge of $H(z)$ is close to $f_s/4$. In the former case, we cannot use $N = 1$ and $M = 2$ at all. In the latter case, the transition bands of $H_D(z)$ and $H_I(z)$ become narrow, resulting in high filter orders. To avoid this problem, one alternative is to use the building block of Fig. 2(a) with $N = 3$ and $M = 2$. In this case, the input-output relation is

$$V(z) = F_1(z)X(z^3) + F_2(z)X(-z^3) \quad (8a)$$

$$Y(z) = V(z^{1/3}) + V(z^{1/3}e^{j2\pi/3}) + V(z^{1/3}e^{j4\pi/3}), \quad (8b)$$

where $F_1(z)$ and $F_2(z)$ are given by Eqs. (2b) and (2c), respectively. In this case, the relation between the input of $H_D(z)$ and the output of $H_I(z)$ is the same as in Case A. The basic difference is that the input sampling rate of $H_D(z)$ is now $f_s' = 3f_s$ and the input of $H_D(z)$ contains one and a half periods of the original input signal spectrum [see Fig. 7(a)]. The specifications for the overall filter consisting of the termination filter, the decimator, and the interpolator are the same except that the sampling rate is now $f_s' = 3f_s$ [see Fig. 7(b)]. The second basic difference compared to Case A is that there are also aliased terms when finally decimating by three, as shown by Eq. (8b). However, because of filtering, the components aliased from the region $[f_s/2, 3f_s/2]$ are very small [see Fig. 7(c)].

The sampling frequency of the center filter $\hat{H}(z)$ is in this case $\hat{f}_s = 3/2f_s$, i.e., $3/2$ times that of the overall filter $H(z)$. The advantage of using $r = 2/3$ lies, however, in the following facts. First, the edges for the half-band designs of $H_D(z)$ and $H_I(z)$ are $f_p^{(D)} = f_c + \Delta/3$ and $f_{st}^{(D)} = f_s'/2 - (f_c + \Delta/3)$. Therefore, the relative transition bandwidth is very wide, resulting in very low filter orders. Second, the passband and stopband edges of $\hat{H}(z)$ are close to $\hat{f}_s/3$ so that the design procedure can be easily repeated using the building block of Fig. 2(a) with $N = 1$ and $M = 2$.

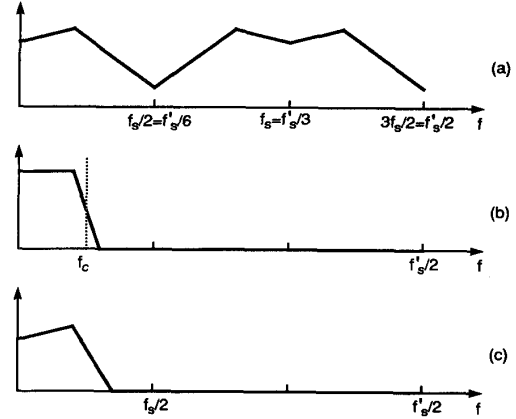


Fig. 7. Filtering in Case C. (a) Periodic input signal spectrum of $H_D(z)$. (b) Transfer function from the input of $H_D(z)$ to the output of $H_I(z)$. (c) Output signal spectrum of $H_I(z)$ before sampling rate reduction by 3.

It can be shown that by ignoring the aliased terms, the passband and stopband ripples of the overall design are at most

$$\delta_p = \sum_{k \in S} 2\delta^{(k)} + \hat{\delta} \quad (9a)$$

$$\delta_s = \sum_{k \notin S} 2\delta^{(k)} + \tilde{\delta}, \quad (9b)$$

where $\delta^{(k)}$ is the ripple of the k th decimator and interpolator and S is the set of stages in front of which there is an even number of building blocks of Fig. 2(b) or no blocks. $\hat{\delta}$ ($\tilde{\delta}$) is the passband (stopband) ripple of the termination filter if there is an even number of delay blocks in front of it. Otherwise, it is the stopband (passband) ripple. The simplest way to determine the required ripples is to make all the terms in the summations equal.

V. DESIGN EXAMPLES

As an example we consider the design of a lowpass filter with passband and stopband edges of $0.2f_s$ and $0.201f_s$ $[(0.2005 \pm 0.0005)f_s]$ and passband and stopband ripples 0.001 (60-dB attenuation). The minimum order of a conventional direct-form design to meet these criteria is 3256, requiring 1629 multiplications per input sample. Using the synthesis procedure described in the previous sections, the first building block is selected to be the one in Fig. 2(a) with $N = 1$ and $M = 2$. The edges of the termination filter are, in terms of its sampling rate $f_s^{(1)} = f_s/2$, $(0.401 \pm 0.001)f_s^{(1)}$. The passband edge for both $H_D(z)$ and $H_I(z)$ is $(0.2005 + 0.0005/3)f_s$. The termination filter is now wideband. Therefore, we use the building blocks of Figs. 2(b) and 2(a). The edges of the termination are $(0.198 \pm 0.002)f_s^{(2)}$ where $f_s^{(2)} = f_s/4$ is its sampling rate. $H_D(z)$ and $H_I(z)$ are highpass half-band filters with stopband edge of $(0.099 + 0.001/3)f_s^{(1)}$. Proceeding in the same manner, the sampling rates for the third, fourth, fifth and sixth terminations become $f_s^{(k)} = f_s/2^k$ for $k = 3, 4, 5, 6$. For the third and fifth stages, we use the building block of Fig. 2(a) with $N = 1$ and $M = 2$ and the passband edges of the subfilters are $(0.198 + 0.002/3)f_s^{(2)}$ and $(0.208 + 0.008/3)f_s^{(4)}$, respectively. For the fourth and sixth stages, we use the building blocks of Figs. 2(b) and 2(a) with $N = 1$ and $M = 2$. The subfilters are highpass half-band filters with stopband edges of $(0.104 + 0.004/3)f_s^{(3)}$ and $(0.084 + 0.016/3)f_s^{(5)}$, respectively. If four or six stages are used, the edges of the remaining terminations are $(0.208 \pm 0.008)f_s^{(4)}$ and $(0.168 \pm 0.032)f_s^{(6)}$, respectively. In the case of four stages, the ripples for all the stages become 0.0002 when determined from Eq. (9) in such a way that all the

terms in the summations become equal. In the case of six stages, the ripples are $0.001/7$.

Filter Complexity

With four stages the number of multipliers (the filter orders) for the decimation and interpolation stages are 11 (42), 4 (14), 11 (42), and 4 (14). The implementation of all the decimators and interpolators requires 16.25 multiplications per input sample. The minimum order of a direct-form FIR filter to meet the criteria of the termination is 264. This filter requires 133 multipliers. Since it is working at the sampling rate of $f_s/16$, it requires 8.3125 multiplications per input sample. The overall multiplication rate is thus 24.5625. For the first building block of Fig. 2(b), the delay term is z^{-1210} and, for the second block, z^{-278} . The number of delay elements required in implementing the overall filter is 1864, which is lower than that for the direct-form design (3256). The delay for the unaliased component is 2462, whereas the delay of the direct-form equivalent is 1628. The multiplication rate can be reduced by designing the termination as an IFIR filter in the form $F(z^2)G(z)$ [1]. The required orders of $F(z)$ and $G(z)$ are 136 and 12, respectively. In this case, the overall multiplication rate is 21.

When six stages are used, then the number of multipliers (orders) for the decimators and interpolators become 12 (46), 4 (14), 11 (42), 4 (14), 15 (58), and 4 (14). The order of the termination is 70. The overall multiplication rate is in this case 18.875. The price paid for the reduction in the multiplication rate is the increased overall delay (3970) and the increased number of delay elements (2700).

Aliasing Noise

When four stages are used, then the overall output can be written in the form

$$Y(e^{j\omega}) = \sum_{k=0}^{15} H_k(e^{j\omega}) X(e^{j(\omega-2k\pi/16)}),$$

so that there is an unaliased component and 15 aliased components. Figure 8(a) gives, in the case where the termination is synthesized in the form $F(z^2)G(z)$, $|H_0(e^{j\omega})|$ in dB (amplitude response for the unaliased component). Figure 8(b), in turn, gives $|H_8(e^{j\omega})|$ (solid line), $|H_6(e^{j\omega})|$ (dashed line), and $|H_4(e^{j\omega})|$ (dot-dashed line). The minimum attenuations for these responses are 74 dB, 74 dB, and 83 dB, respectively. For the other responses, the minimum attenuation is more than 86 dB.

Another way of assessing the noise contribution due to aliasing is by simulation with a stochastic input. When the same stochastic signal is input to a multirate filter and to the corresponding time-invariant filter (filter giving only the unaliased output), the aliasing noise can be found as the difference between the two output signals. This simulation with a white input signal, yields for the 4-stage system using an IFIR terminating filter a signal-to-aliasing-noise ratio of 73.1 dB referenced to the 0-dB output level of the signal passband. The non-white noise spectrum is shown in Fig. 9. When comparing this figure with Fig. 8(b), it is seen that the spectrum of Fig. 9 is basically due to the components shown in Fig. 8(b).

Multiplication Rate as a Function of Cutoff Frequency

In order to examine how the multiplication rate varies as a function of the center of the transition band, Fig. 10 is provided. It plots a case where the width of the transition band is $0.001f_s$ and the passband and stopband ripples are, as in the previous example, 0.001. In constructing this plot, the upper allowable number of stages has been fixed to be 8 and the upper limit for the overall delay has been two and a half times that of the direct-form equivalent (4070). As seen from the figure, the maximum number of multiplications per input sample is in this case 40.

VI. FINITE WORDLENGTH EFFECTS

Two effects of finite register lengths have to be considered in FIR systems: the effect of coefficient rounding on the frequency response of the system and noise generation due to internal signal rounding.

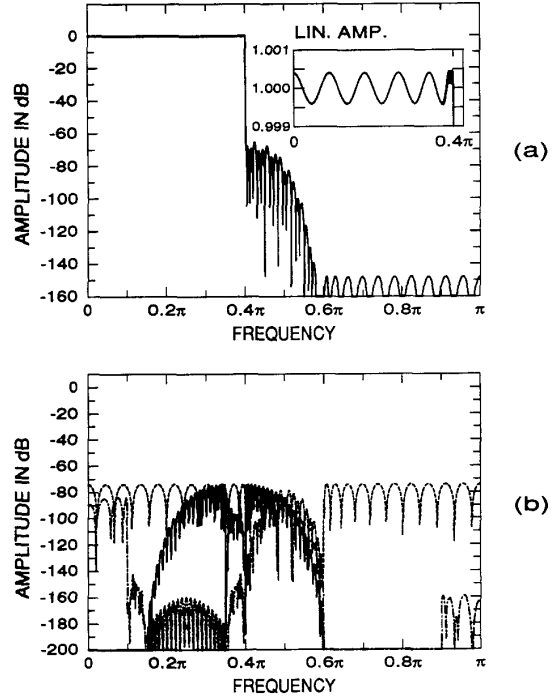


Fig. 8. Responses for the proposed multirate filter with four decimation and interpolation stages. (a) Response for the unaliased component. (b) Responses for some aliased components.

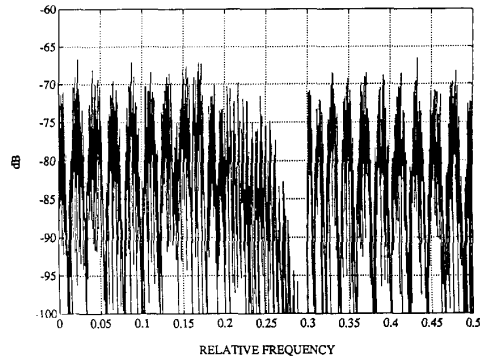


Fig. 9. DFT spectrum of the alias output signal component from the 4-stage system with IFIR terminal filter based on 5000 samples. Input signal: white noise, 0 dB.

Coefficient Sensitivity

When the coefficients in our system are rounded, it affects each individual subfilter. If the subfilter responses are preserved within our specification, so will the overall response.

In order to compare our filters with direct-form filters, we estimate the necessary number of bits in the two systems using the statistical approach given in [8]. From equations (40) and (41) in that paper we find that the frequency response error is with high probability less than

$$\sigma_e \approx 2^{-(t-1)} \sqrt{(2N+1)/3}, \quad (10)$$

where t is the total number of bits and N is the filter order. We now solve for the number of bits and apply the equation to both filters

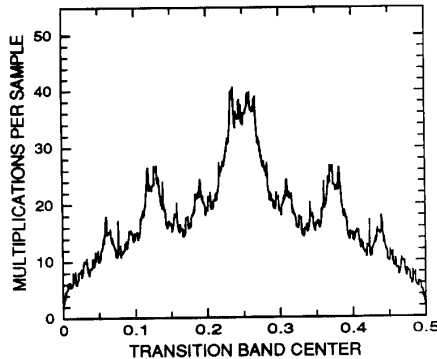


Fig. 10. Multiplication rate versus the center of the transition band for filters with transition band width of $0.001f_s$ and passband and stopband ripples of 0.001.

under investigation, inserting indexes d and m for the multirate and direct-form filters, respectively. Assuming that the relative allowable error in the stopband due to coefficient quantization is the same for both filters ($\sigma_s = \alpha\delta, \alpha < 1$) we obtain, after some manipulation, for the difference in the number of coefficient bits,

$$t_d - t_m = 0.5 \log_2(N_d/N_m) - \log_2(\delta_d/\delta_m), \quad (11)$$

where δ_d and δ_m are the stopband ripples. To simplify the equation we have here assumed that N is large for both filters.

Applying Eq. (11) to compare the direct-form filter with $\delta_d = 0.001$ order of 3256 with the terminating filter of the 6-stage design having $\delta_m = 0.001/7$ and order 70, one finds that the two filters require approximately the same number of bits.

One may expect this result to be quite general, because on one hand, the multirate system has stricter inband tolerances, while on the other hand, the filter order of the direct-form filter is higher, each pulling in different directions.

Quantization Noise

Space limitations do not allow a detailed noise analysis. We will therefore rather present a qualitative discussion and give a SNR for our example compared with a direct-form filter meeting the same specifications.

To evaluate the effects of representing the internal signals by a finite number of bits, we have employed the following model: We assume that all adders have a sufficient number of bits to avoid any significant contribution both to quantization noise and saturation effects. At the output of all filters and after the additions of the delay line outputs and the interpolating filter outputs, there are scaling multipliers followed by quantizers. The scaling multipliers amplify the signals as much as possible without bringing it to saturation. The quantizers round the signal to the required number of bits.

It is not hard to realize that the noise at the filter output will be non-white due to the number of noise sources influencing the various frequency regions. The transfer function from the terminating filter and those close to it will basically have a bandpass character with the passband at the edge of the overall filter system passband. Therefore, we will expect that the noise will grow towards the passband edge for lowpass filters.

In our simulation experiment we have used a white Gaussian zero-mean unit-variance signal source. All the signal levels have been scaled to unit variance where applicable. The exception is at the external summation points where the signals to be added from the different branches must be scaled by exactly the same total amount. Assuming that the signals at all quantization points are Gaussian, we fix the saturation levels at six times the signal variance.

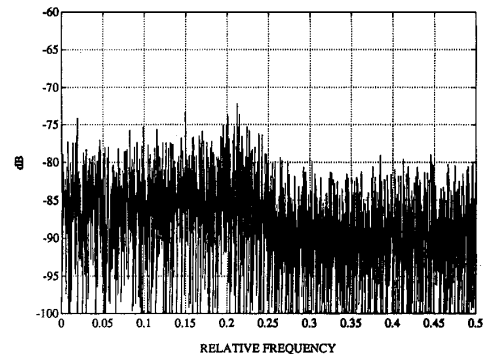


Fig. 11. DFT spectrum of simulated quantization noise in the six-stage structure with 16 internal bits based on 5000 samples. Input signal: white noise, 0 dB.

In our example using the above described scheme and a 16-bit signal representation, one obtains a 78.5 dB signal-to-quantization noise ratio. In Fig. 11 the noise spectrum is shown. As expected, the noise level increases towards the passband edge. To reduce this effect, one might resort to using more bits in the filters close to the center of the structure as compared to the other ones.

To appreciate this result, we have compared it to the noise in a direct-form design using the same input and output scaling. The resulting signal-to-quantization-noise is 80.4 dB when all additions are performed prior to output scaling and quantization. In other words, to obtain the same SNR, we need at most one extra bit in our system for internal signal representation.

VII. CONCLUSION

In this paper we have demonstrated that FIR filters can be implemented with low computational complexity in a structure based on multirate filters. A comparison with IIR filters will reveal that for filters with tight filter specifications these FIR structures will require less computations, but the delay and the memory will, of course, be much larger. We feel that this is a strong demonstration of the efficiency possible in time-varying systems as compared to shift-invariant systems.

REFERENCES

- [1] T. Saramäki, Y. Neuvo, and S. K. Mitra: "Design of computationally efficient interpolated FIR filters," *IEEE Trans. Circuits Syst.*, vol. CAS-35, pp. 70-88, Jan. 1988.
- [2] L. R. Rabiner and R. E. Crochiere, "A novel implementation for narrow-band FIR digital filters," *IEEE Trans. Acoust., Speech, Signal Processing*, vol. ASSP-23, pp. 457-464, Oct. 1975.
- [3] Z. Jing and A. T. Fam, "A new structure for narrow transition band, lopass digital filter design," *IEEE Trans. Acoust., Speech, Signal Processing*, vol. ASSP-32, pp. 362-370, April 1984.
- [4] Y. C. Lim, "Frequency-response masking approach for the synthesis of sharp linear phase digital filters," *IEEE Trans. Circuits Syst.*, vol. CAS-33, pp. 357-364, Apr. 1986.
- [5] T. A. Ramstad and T. Saramäki, "Efficient multirate realization for narrow transition-band FIR filters," in *Proc. 1988 IEEE Int. Symp. Circuits Syst.* (Espoo, Finland), pp. 2019-2022, June 1988.
- [6] M. G. Bellanger, J. L. Daguët, and G. P. Lepagnol, "Interpolation, extrapolation, and reduction of computation speed in digital filters," *IEEE Trans. Acoust., Speech, Signal Processing*, vol. ASSP-22, pp. 231-235, Aug. 1974.
- [7] R. E. Crochiere and L. R. Rabiner, *Multirate Digital Signal Processing*. Englewood Cliffs, NJ: Prentice-Hall, 1983.
- [8] D. S. K. Chan, L. R. Rabiner: "Analysis of quantization errors in the direct form for finite impulse response digital filters," *IEEE Trans. Audio Electroacoust.*, vol. AU-21, pp. 354-366, August 1973.